Bulletin of the Seismological Society of America, Vol. 88, No. 5, pp. 1171–1181, October 1998

Implications of a Composite Source Model and Seismic-Wave Attenuation for the Observed Simplicity of Small Earthquakes and Reported Duration of Earthquake Initiation Phase

by S. K. Singh, M. Ordaz, T. Mikumo, J. Pacheco, C. Valdés, and P. Mandal

Abstract An examination of P waves recorded on near-source, velocity seismograms generally shows that most small earthquakes ($M_w < 2$ to 3) are simple. On the other hand, larger earthquakes ($M_w \geqq 4$) are most often complex. The simplicity of the seismograms of $M_w < 2$ to 3 events may reflect the simplicity of the source (and, hence, may imply that smaller and larger earthquakes are not self-similar) or may be a consequence of attenuation of seismic waves. To test whether the attenuation is the cause, we generated synthetic P-wave seismograms from a composite circular source model in which subevent rupture areas are assumed to follow a power-law distribution. The rupture of an event is assumed to initiate at a random point on the fault and to propagate with a uniform speed. As the rupture front reaches the center of a subevent patch (all of which are circular), a P pulse is radiated that is calculated from the kinematic source model of Sato and Hirasawa (1973). Synthetic P-wave seismograms, which are all complex, are then convolved with an attenuation operator for different values of t^*. The results show that the observed simplicity of small events ($M_w < 2$ to 3) may be entirely explained by attenuation if $t^* \geqq 0.02$ sec.

The composite source model predicts that the average time delay between the initiation of the rupture and the rupture of the largest patch, τ, scales as $M_0^{1/3}$, such that $\log \tau = (1/3) \log M_0 - 8.462$. This relation is very similar to that reported by Umeda *et al.* (1996) between M_0 and the observed time difference between the initiation of the rupture and the rupture of the "bright spot." It roughly agrees with the relation between M_0 and the duration of the initiation phase reported by Ellsworth and Beroza (1995) and Beroza and Ellsworth (1996). The relation also fits surprisingly well the data on duration of slow initial phase, $t$sip, and M_0, reported by Iio (1995). One possible explanation of this agreement may be that the composite source model, which is essentially the "cascade" model, successfully captures the evolution of the earthquake source process and that the rupture initiation and the abrupt increase in the velocity amplitude observed on seismograms by previous researchers roughly corresponds to the rupture of the first subevent and the breaking of the largest subevent in the composite source model.

Introduction

There is consensus that the ω^2 scaling of seismic source spectrum with constant stress drop, as proposed by Aki (1967), is, generally, valid for earthquakes over a wide range of magnitude. This scaling implies that the earthquakes are self-similar. The validity of the Gutenberg–Richter relationship, $\log N = a - bM$, with $b = 1$, is also consistent with this scaling (Hanks, 1979; Andrews, 1981). The validity for small earthquakes, however, remains controversial. Some studies find that the stress drop of small earthquakes decreases with seismic moment (e.g., Archuleta *et al.,* 1982), while others report that it remains constant for such events (e.g., Abercrombie, 1995). Also, a decrease in the b-value for $M < 2$ to 3, unrelated to the completeness of earthquake catalog, has been reported in some studies (e.g., Aki, 1987; Umino and Sacks, 1993), but no such change has been found in others (e.g., Abercrombie, 1996).

An observation, which also has bearing on self-similarity of earthquakes, is the relative simplicity of most near-

source velocity seismograms of small ($M_w < 2$ to 3) earthquakes recorded on the Earth's surface. Here we define an event as *simple* if the first *P*-wave cycle, recorded on the vertical component, is the largest and shows no visual evidence of complexity in the first half of the cycle. We inquire whether this is due to the source characteristics of such events or is a consequence of the attenuation. If small earthquake sources are simple and large earthquakes are complex, then small and large are not self-similar, which, if true, would have a major impact on our understanding of scaling of earthquakes. If attenuation can explain the observed simplicity, then it would mean that the complexity and simplicity of small earthquakes cannot be resolved by the available data. To test the effect of attenuation, we generate synthetic *P*-wave seismograms from a composite circular-source model. Synthetic *P*-wave seismograms, which are all complex, are convolved with an attenuation operator involving reasonable values of t^*. The resulting seismograms are then examined to know the effect of attenuation on the complex seismograms.

Our result has some implications for the initiation and the evolution of earthquake rupture, a topic of much current interest in seismology. It has been suggested that the rupture initiation may contain information regarding the eventual size of the earthquake (Matsu'ura *et al.,* 1992; Sibazaki and Matsu'ura, 1992; Iio, 1992a, 1995; Ellsworth and Beroza, 1995; Beroza and Ellsworth, 1996). If the attenuation drastically changes the waveform of small earthquakes, then it may be difficult to know the true nature of rupture initiation, a conclusion previously reached by Mori and Kanamori (1996).

It has been reported that the time difference between rupture initiation and the rapid increase of velocity amplitude observed in seismograms scales with seismic moment, M_0, of the event (Iio, 1992a, 1995; Umeda, 1992; Umeda *et al.,* 1996; Ellsworth and Beroza, 1995; Beroza and Ellsworth, 1996). We intuitively expect that in the composite source model, the time delay, τ, between the initiation of the rupture and the rupture of the largest patch would scale with M_0. In this study, we explore this scaling in detail and compare it with those previously reported.

Data

Simplicity of small earthquakes recorded on the Earth's surface can be seen in several publications (see, e.g., Figs. 4 and 22 of Iio, 1995; Fig. 7 of Beroza and Ellsworth, 1996). Some more examples, showing relative simplicity of small earthquakes on near-source, *Z*-component velocity seismograms, are given in Figures 1 to 3. We note that the selection of small earthquakes in these figures is random. These recordings were either made by accelerographs (flat response for acceleration from DC up to about the natural frequency of the sensor, which is ~50 Hz) or by broadband (BB) seismographs (flat response for velocity from about 50 sec to up to about 50 Hz or roughly about 80% of the Nyquist frequency, whichever is smaller). The acceleration traces were integrated once to obtain velocity seismograms. The broadband traces were corrected for the gain factor (counts cm^{-1} sec^{-1}) only. No further corrections were applied. The characteristics of the instruments recording the events are briefly described below.

Figure 1 shows epicentral seismograms (*S-P* time ~0.6 sec) of an earthquake swarm that occurred near the town of Zacoalco, Jalisco, Mexico, in May 1997. The events were recorded by 24-bit RefTek digitizers connected to Guralp CMG-40T sensors. The sampling rate was 250 Hz. The velocity response of CMT-40T is flat between 50 sec and 50 Hz. The Reftek antialiasing filter has a cutoff at 85% of the Nyquist, with 120 dB down at the output Nyquist frequency. With the possible exception of one earthquake, all events, which cover a range of $0.9 \leqq M_w \leqq 2.5$, are simple, and the amplitude of the first cycle of the *P* wave scales with M_w.

In Figure 2, we show seismograms (*S-P* times ~3.2 sec) of the mainshock of the 15 July 1996 earthquake (M_w =

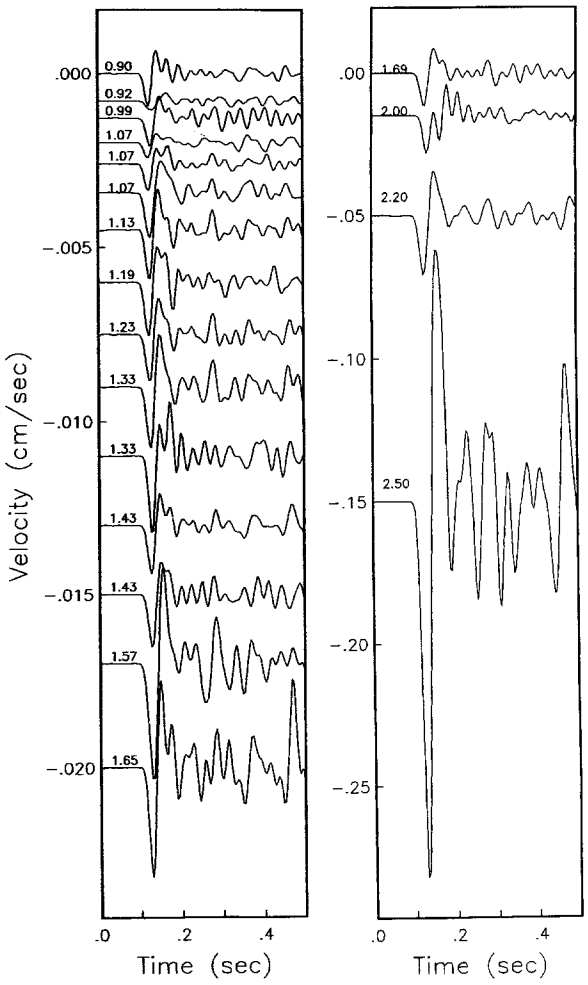

Figure 1. Near-source vertical seismograms (*S-P* time ~0.6 sec, sampling rate = 250 Hz) of an earthquake swarm that occurred near the town of Zacoalco, Jalisco. Mexico, in May 1997.

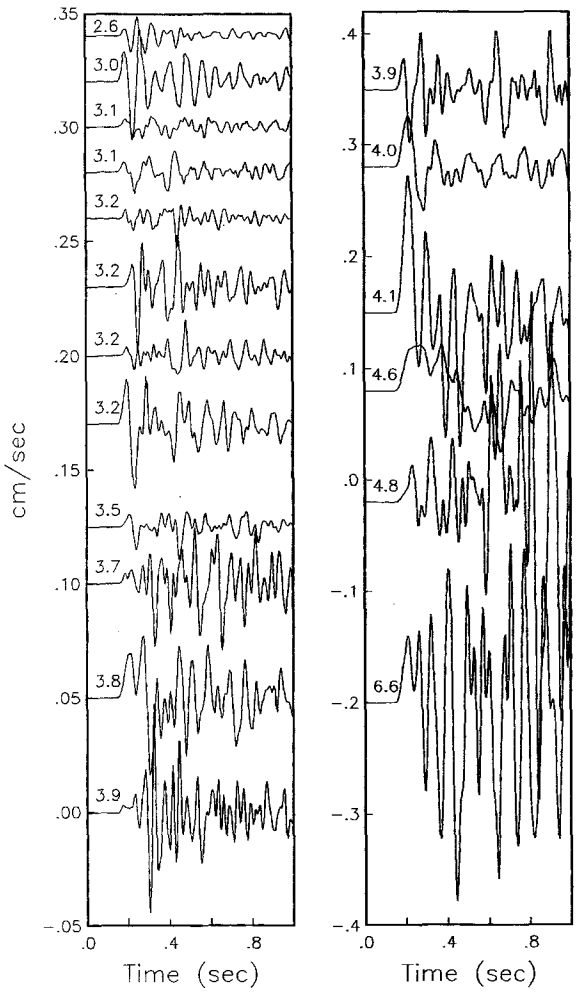

Figure 2. Near-source vertical seismograms (*S-P* times ~ 3.2 sec, sampling rate = 200 Hz) of the mainshock of the 15 July 1996 earthquake (M_w = 6.6), which occurred near the town of Papanoa, Mexico, and its aftershocks. These events were recorded on a 19-bit accelerograph. The traces given in the figure were obtained by direct integration of the accelerograms.

6.6), which occurred near the town of Papanoa, Mexico, and its aftershocks ($2.6 \leqq M_w \leqq 4.8$). These events were recorded by a 19-bit Kinemetrics K2 accelerograph at Papanoa with a sampling rate of 200 Hz. Antialiasing in K2 is achieved by a Brickwall FIR filter, with cutoff at 80% of output Nyquist and 120 dB down at the output Nyquist frequency. The sensor has a natural frequency of 50 Hz. The acceleration response is flat from DC to about 45 Hz. The traces given in the figure were obtained by direct integration of the accelerograms. Five out of nine $M_w \leqq 3.5$ events are simple. Of the nine earthquakes with $M_w > 3.5$, only two (M_w = 3.9 and 4.0) may qualify as simple events.

Figure 3 shows a compilation of near-source seismograms (*S-P* times about 3 to 4 sec, $3.0 \leqq M_w \leqq 8.0$) from different stations above the Mexican subduction zone. The data at the station CAIG were recorded on a BB seismograph (STS-2 seismometer connected to 24-bit Quanterra digitizer, sampling rate 80 Hz). The response of the BB system is flat from about 50 sec to 35 Hz. All other events were recorded by accelerographs (FBA accelerometers with natural frequency of 50 Hz; 12-, 19-, or 24-bit digitizers; sampling rate 80, 100, or 200 Hz). The seismograms sample different parts of the focal sphere and include the effect of local geology, which is expected to differ for each site. The events with $M_w \leqq 5.0$ have been randomly selected. The direct integration of near-source accelerograms, recorded by 12-bit digitizers, often yield velocity seismograms that are not realistic. In Figure 3, we include all those $M_w > 5.0$ events that gave rise to reliable near-source seismograms. An examination of this figure suggests that all earthquakes with $M_w \geqq 4.4$ are complex, whereas the smaller events ($3.0 \leqq M_w \leqq 4.3$) are simple as well as complex.

From Figures 1 to 3, taken together, we conclude that (a) the near-source *Z*-component seismograms of most $M_w < 2$ to 3 earthquakes are simple and the amplitude of the *P*-wave cycle scales with M_w; (b) for events with $3 < M_w < 4.5$, the seismograms are simple as well as complex, and the amplitude of the *P* wave still roughly scales with M_w, and (c) these seismograms are complex for almost all $M_w \geqq 4.5$, and the amplitude of the initial part of the seismogram does not scale with M_w. The conclusion (*c*) is similar to that reached by Singh *et al.* (1989) and Anderson and Chen (1995), who examined the accelerograms from the Mexican subduction zone.

Is the Source or the Attenuation the Cause of the Simplicity?

One possible explanation for the observed simplicity of the seismograms of small earthquakes may be the simplicity of the sources, that is, smooth rupture propagation over the fault area of such events. Because it is well known that large earthquakes are complex, the simplicity of small earthquakes would imply that small and large earthquakes are not self-similar. Another possible explanation may be that small earthquakes are just as complex as the large ones, but the limited bandwidth of the recording system and the attenuation causes the complex waveforms to be reduced to simple ones. In this section, we assume that small earthquakes are complex and evaluate the effect of attenuation on the waveforms. As shown below, we find that in most cases this effect alone is sufficient to make the complex seismograms of small earthquakes ($M_w < 2$ to 3) appear simple.

The complexity of the earthquake source may come either from heterogeneous distribution of fault strength (e.g., Das and Aki, 1977; Mikumo and Miyatake, 1978; Miyatake, 1980, Day, 1982. Papageorgiou and Aki, 1983; Mikumo and Miyatake, 1987) and nonuniform stress drop on the fault plane (e.g., Mikumo and Miyatake, 1995) or from the existence of nonplanar cracks parallel to the main fault (e.g., Yamashita and Umeda, 1994; Umeda *et al.* 1996). From the dynamic point of view, it would be necessary to solve elas-

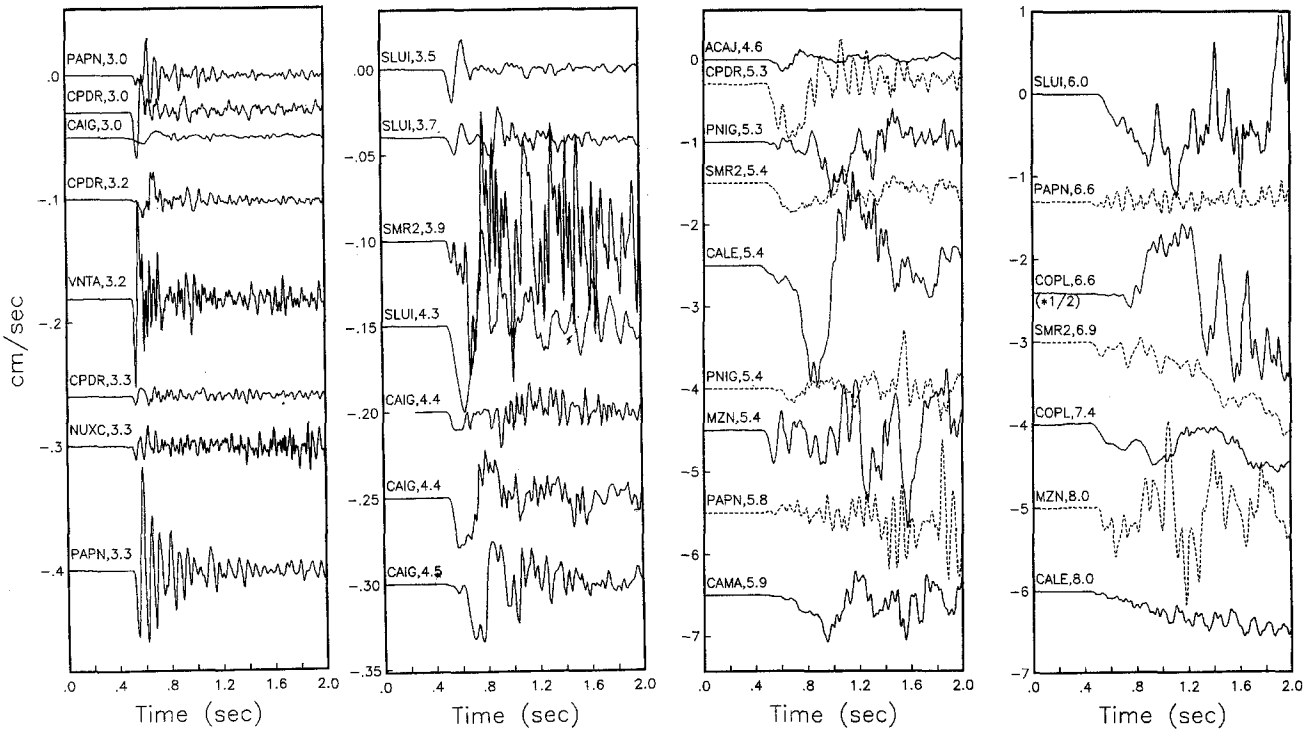

Figure 3. A compilation of near-source seismograms (*S-P* times about 3 to 4 sec) from stations above the Mexican subduction zone. Some of these events were recorded by accelerographs and others by BB seismographs.

todynamic equations incorporating these heterogeneities in order to calculate seismic waveforms at any observation point. However, any model that can generate sufficiently complex waveforms would serve our purpose here. For this reason, and the fact that it is simple to implement, we will use a composite kinematic source model, instead of the dynamic models, to generate synthetic seismograms.

Synthetic Seismograms from a Composite Source Model

We assume that the faulting process of an earthquake can be idealized by a composite kinematic source model. We use a slightly modified version of the composite source model given by Zeng *et al.* (1994), which, in turn, is based on a self-similar model proposed by Frankel (1991). In our model, the final rupture area is assumed circular of radius R. This rupture area is filled with circular subevents of radius r (the subevents are allowed to overlap), which is a random variable with truncated fractal distribution (also known as Pareto's distribution) of parameter D. The corresponding probability density function is

$$p_r(r) = \frac{D}{R_{\min}^{-D} - R_{\max}^{-D}} r^{-(D+1)}, \quad R_{\min} \leqq r \leqq R_{\max}.$$

We take $R_{\max} = R$. The fractal dimension D is taken as 2 (Frankel, 1991).

We want to simulate a source with a seismic moment M_0. This moment should equal the sum of the moments of the subevents:

$$M_0 = \sum_{i=1}^{N} M_0^i = \frac{16}{7} \Delta\sigma \sum_{i=1}^{N} r_i^3.$$

In view of this, the expected number of subevents $E(N)$ to match a target seismic moment M_0 is given by (Zeng *et al.*, 1994):

$$E(N) = \frac{p}{D} (R_{\min}^{-D} - R_{\max}^{-D}),$$

where

$$p = \frac{7M_0}{16\Delta\sigma} \frac{3 - D}{(R_{\max}^{3-D} - R_{\min}^{3-D})}.$$

To simulate a source with subevent sizes distributed as previously indicated, there are two possible strategies. One is to simulate exactly $E(N)$ subevents. On the average, the sum of the seismic moments of these subevents would be M_0. However, individual realizations of the simulation could yield moments much larger or much smaller than the target moment. Another possibility, which we have used in this study, is to generate as many subevents as necessary to accumulate the desired moment within a pre-established tolerance. To simulate subevent sizes, we use the inverse

method, which requires specification of the probability distributions of subevent sizes, $P_r(r)$:

$$P_r(r) = \int_{R_{\min}}^{r} p_r(r)dr = \frac{R_{\min}^{-D} - r^{-D}}{R_{\min}^{-D} - R_{\max}^{-D}},$$

which leads to subevent sizes r_i, given by

$$r_i = [R_{\min}^{-D} - u_i(R_{\min}^{-D} - R_{\max}^{-D})]^{-1/D},$$

where u_i is a uniformly distributed random number between 0 and 1.

In the simulations, we chose $R_{\min} = 0.05R$ and $\Delta\sigma = 30$ bar, unless otherwise mentioned. The point of initiation of the rupture is selected randomly, and the rupture front is assumed to expand with constant speed, V_R. Individual subevents radiate a P pulse when the front reaches its center. The far-field P pulse of an individual subevent is computed using Sato and Hirasawa's (1973) circular source model located in an infinite space. This model may be regarded as a kinematic version of the dynamic circular model of Madariaga (1976). In the computations, the observer is located at 18 km from the center of the rupture area, with $\theta = 30°$, $\phi = 0°$, $\alpha = 6.5$ km/sec, $\beta = \alpha/\sqrt{3}$, rupture velocity $V_R = 0.9\beta$, and $\rho = 2.8$ gm/cm^3. In this case, the P-wave displacement spectrum falls off as $\omega^{-2.05}$ for the Sato and Hirasawa model. The corresponding average spectral falloff for the composite source model is $\omega^{-1.96}$. Thus the synthetics seismograms from the composite source model are slightly more enriched at high frequencies than those from the Sato and Hirasawa model.

In Figures 4 to 8, we illustrate synthetic seismograms ($1.0 \leqq M_w \leqq 3.5$) from the simple circular source model of Sato and Hirasawa and those from six simulations of the composite source model. The attenuation effect was included by convolving the synthetic P waves with Futterman's (1962) attenuation operator for various values of t^*. The figures include seismograms corresponding to $t^* = 0$ (no attenuation), 0.006, 0.02, and 0.03 sec. At a hypocentral distance of 18 km and for $\alpha = 6.5$ km/sec, the values of t^* of 0.006, 0.02, and 0.03 sec correspond to Q_P of 465, 138, and 92, respectively, assuming no near-site attenuation. An examination of Figures 4 to 8 shows that the composite source seismograms remain mostly simple for $M_w \leqq 1.5$ for all values of t^* considered. Events larger than $M_w = 1.5$, 2, and 3 appear complex for $t^* = 0.006$, 0.02, and 0.03 sec, respectively.

We estimated the value of t^* for the region of Zacoalco, Mexico, by comparing stacked normalized waveforms of the recorded events with $M_w \sim 1.1$, with synthetic seismograms from an $M_w = 1.1$ earthquake convolved with the attenuation operator using different values of t^*. This comparison for Zacoalco (Fig. 9) suggests a t^* of 0.04 sec. From this and Figures 4 to 8, it follows that the recorded seismograms

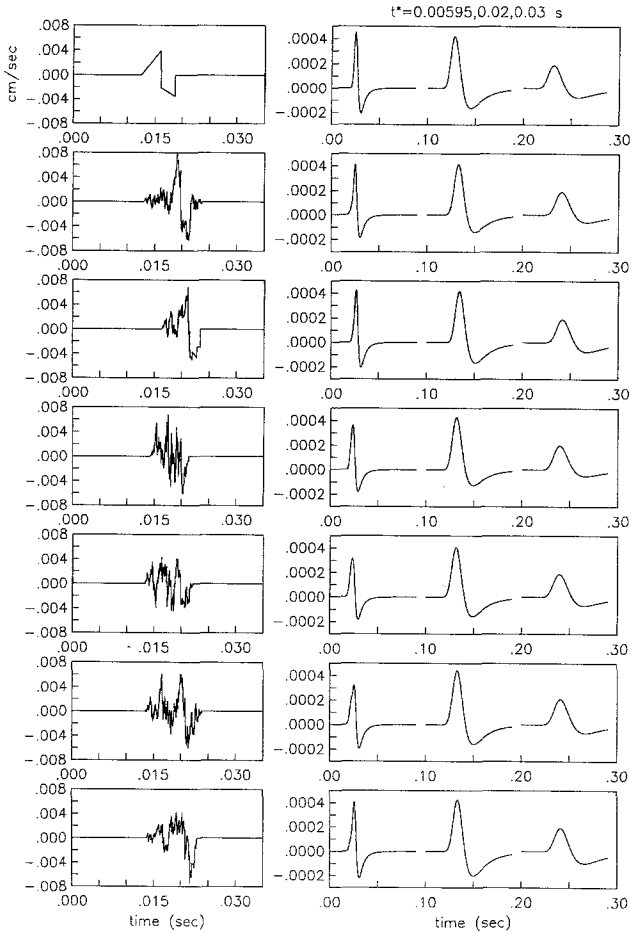

Figure 4. Synthetic near-source vertical seismograms, $M_w = 1$. Left frames show synthetics in the absence of attenuation (top: simple source; the following 6 frames: composite source). The frames on the right give corresponding seismograms for $t^* = 0.006$, 0.02, and 0.03 sec. The seismograms corresponding to $t^* = 0.02$ and 0.03 sec (the last two seismograms on the right-hand frames) have been multiplied by a factor of 8.

for $M_w \leqq 3$ should be simple. This is in agreement with Figure 1. In as much as $t^* \geqq 0.02$ sec is a commonly reported value for near-source recordings (see, e.g., Hough *et al.*, 1988; Mori and Kanamori, 1996), we may conclude that in most cases the attenuation would make complex seismograms look simple for small ($M_w < 2$ to 3) earthquakes. Thus, the observed simplicity of small earthquakes can be explained by attenuation alone. Our study does not rule out that smaller events may, in fact, be simpler than larger ones; it only demonstrates that because of attenuation of seismic waves, it may not be possible to resolve this, unless near-source recordings are made on very competent rocks or in deep boreholes. It is worth noting that the seismograms of small earthquakes recorded at depth are often complex (see, e.g., Beroza and Ellsworth, 1996, Fig. 7).

One dataset for which the reported t^* value is very small

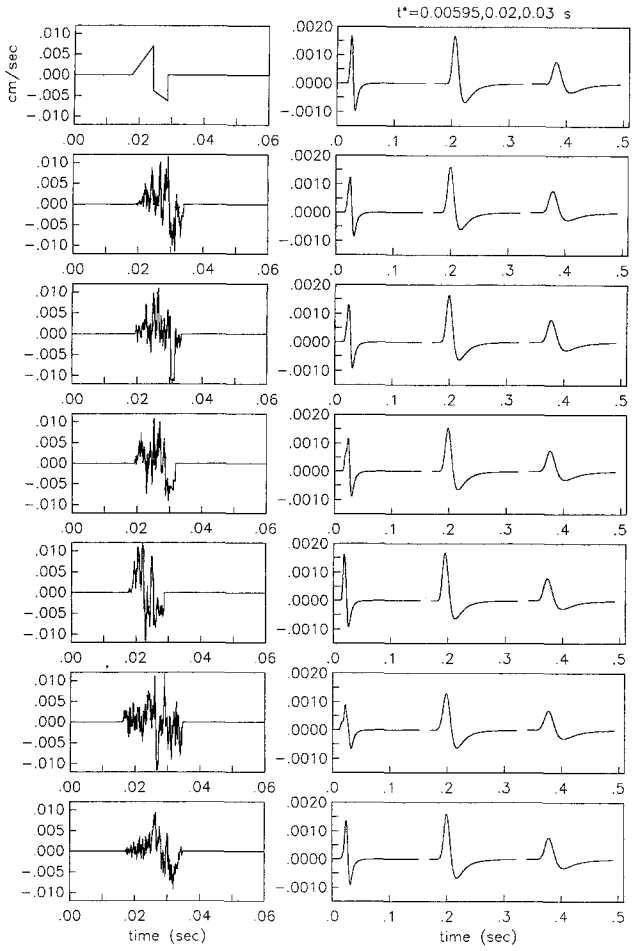

Figure 5. Same as Figure 4 but for M_w = 1.5. The seismograms corresponding to t^* = 0.02 and 0.03 sec have been multiplied by a factor of 6.

comes from the near-source microearthquakes recordings of the aftershocks of the 1984 Western Nagano Prefecture, Japan, earthquake. The microearthquakes ($-0.67 \leqq M_w \leqq 2.67$), analyzed by Iio (1992a, 1995), were recorded on a hard-rock site. Iio (1992a) estimated $Q_P \geqq 280$ from recordings at a distance of about 10 km. For P-wave velocity of 6.0 km/sec (Iio, 1995) and Q_P = 280, t^* is 0.006 sec. Although the events studied by Iio had a focal distance of 0.3 to 12.3 km, 54 of the 69 earthquakes had a focal distance between 7.0 and 12.3 km. In this short distance range, the t^* may be taken as 0.006 sec. Iio (1992a) reports that Q_P = 280 is a lower bound, and, hence, t^* = 0.006 sec is an upper bound. For t^* = 0.006 sec, Figures 5 and 6 predict complex waveforms for $M_w \geqq 1.5$. However, the waveforms given by Iio (1995, see Fig. 4) are all simple. Following are some possible explanations for this discrepancy. (1) The small earthquakes were indeed simple. (2) Dynamically, the total duration of rupture, T, for a circular fault equals R/V_R, where R is the radius of the fault and V_R is the rupture velocity. In the static limit, R is proportional to $(M_0/\Delta\sigma)^{1/3}$, where $\Delta\sigma$ is the stress drop, so that $T \propto R \propto (M_0/\Delta\sigma)^{1/3}$. Thus, higher values of $\Delta\sigma$(>30 bars) of the events would result in smaller values of T for the same M_0. Since the convolved synthetics would then appear simple over a larger-magnitude range, the observed simplicity of the Western Nagano seismograms may be explained by high stress drops during these events. Iio (1992b), however, reports that the source process of the microearthquakes was slow and smooth and involved stress drop between 0.1 and 1 bar. Thus either (1) above is the correct explanation or, else, Iio (1992b) has not adequately considered the local site effects. It is well known that even "hard-site" recordings are affected by attenuation and scattering caused by joints and fractures in the near-surface weathered zone (e.g., Cranswick *et al.*, 1985). It is also very likely the case with Iio's data; however, the quantification of this effect is beyond the scope of this article.

The results of this section emphasize that any fine features of the rupture initiation may be lost due to attenuation unless the correction for it can be made with great accuracy.

Scaling of the Duration of the Initiation Phase with Seismic Moment

It has been reported by Umeda (1990, 1992) that a relatively low-amplitude P phase precedes the main energy release (corresponding to the rupture of a "bright" spot) during moderate and large earthquakes ($M > 5.0$) and that the duration between the two episodes scales with magnitude of the earthquake. Umeda *et al.* (1996) suggest that the beginning of the initial phase corresponds to the end of the quasi-static process and the start of the quasi-dynamic one. These authors attribute the occurrence of the bright spot to the non-coplanar interaction of pre-existing cracks at some distance from the hypocenter and to excitation of the dynamic slip on the main crack surface. Umeda (1990) noted that the initial phase is not seen for aftershocks and swarm type of earthquakes, and Umeda *et al.* (1996) suggested temporal change in the fault-zone properties or medium heterogeneities as the cause of this difference. Iio (1992a, 1995), Ellsworth and Beroza (1995), and Beroza and Ellsworth (1996), as also Matsu'ura *et al.* (1992) and Shibazaki and Matsu'ura (1992), find that the dynamic rupture during an earthquake is preceded by a nucleation phase (during which the rate of moment release is relatively low) and that the duration of this phase scales with the eventual size of the earthquake. Although the measurements of the delay between the initiation of the rupture and the rapid increase of velocity amplitude from seismograms reported by Umeda (1990, 1992), Ellsworth and Beroza (1995), and Beroza and Ellsworth (1996) seem to be somewhat subjective and may be difficult to make on some seismograms, there is little doubt that there is a delay, τ. It is also difficult to dismiss the observation that τ scales with $M_0^{1/3}$. However, no satisfactory model has been put forward to explain this scaling.

In the composite circular source model previously outlined, the rupture almost always begins with the breakage of a small subevent. This is because we allow the rupture areas

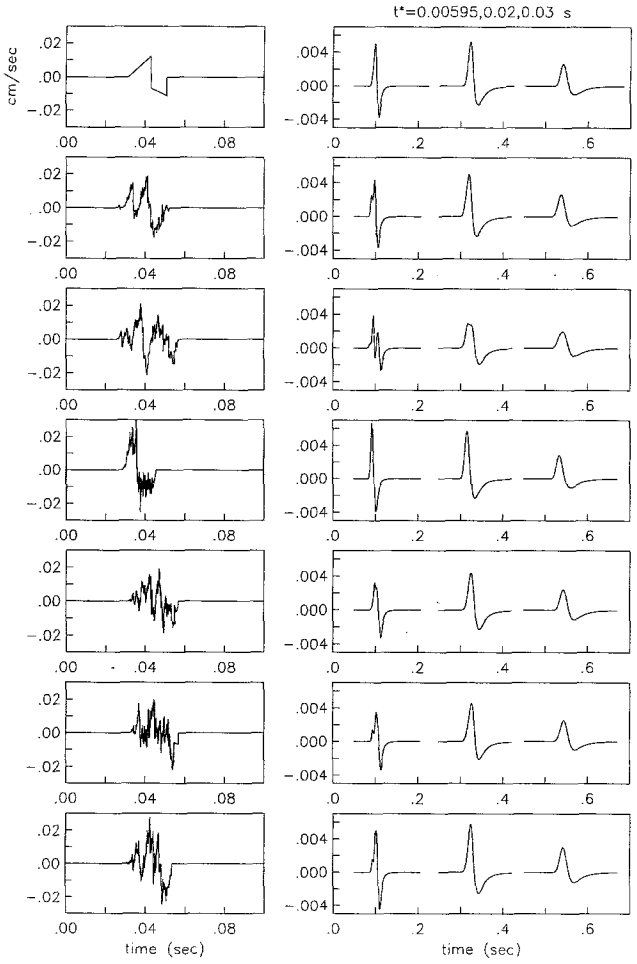

Figure 6. Same as Figure 4 but for M_w = 2.0. Factor of multiplication of seismograms corresponding to t^* = 0.02 and 0.03 sec is 4.

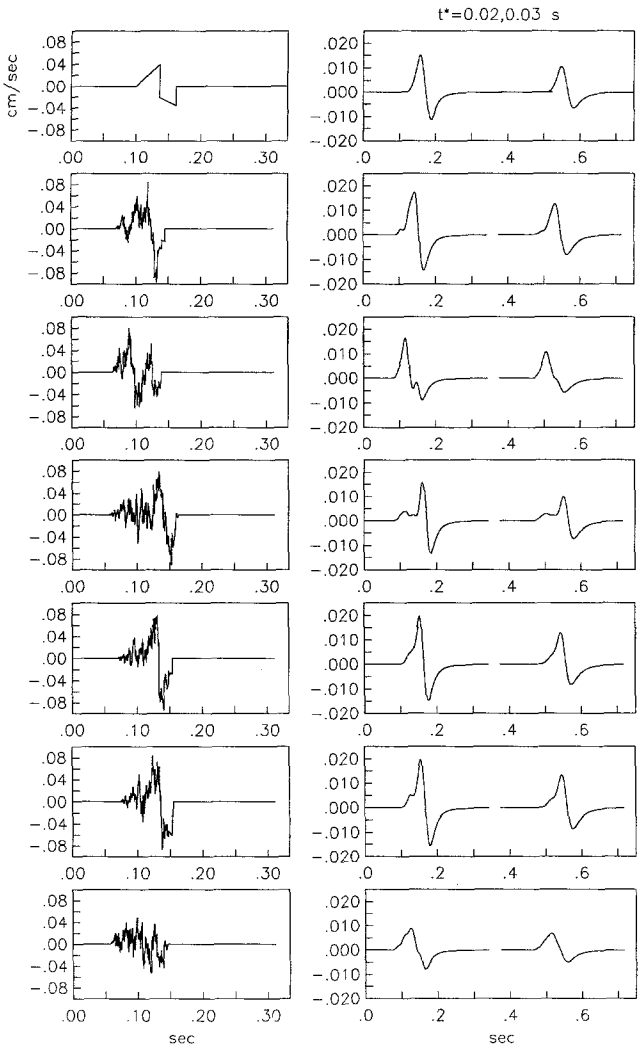

Figure 7. Same as Figure 4 but for M_w = 3.0. The seismograms corresponding to t^* = 0.006 sec is not shown.

of the subevents to overlap. The first subevent to rupture is one whose center is closest to a random point on the plane. We carried out 80 simulations for each magnitude to obtain the time difference in the rupture initiation and the rupture of the largest subevent. This delay, τ, is shown in Figure 10 as a function of M_0. As seen in the figure, the median value of τ scales as $M_0^{1/3}$, such that $\log \tau = (1/3) \log M_0 - 8.462$. The scaling is a consequence of the fact that, on an average, τ equals some fraction of total rupture time T, so that $\tau = CT = CR/V_R$, where C is a constant. Because $M_0 = (16/7)\ \Delta\sigma\ R^3$ (Keilis-Borok, 1959), we can write

$$\tau = C\ R/V_R = (C/V_R)(7M_0/16\Delta\sigma)^{1/3}.$$

As mentioned earlier, the composite source model (for $V_R = 0.9\beta = 3.38$ km/sec, and $\Delta\sigma = 30$ bars) predicts that, on an average, $\log \tau = (1/3) \log M_0 - 8.462$. It follows that $C = 0.41$. In other words, on an average, the distance between the point of rupture initiation and the center of the largest subevent is about 0.4 of the radius of the total rupture area.

As seen from Figure 11, the predicted relationship between τ and M_0 from the composite source model is remarkably similar to that reported by Umeda *et al.* (1996) and roughly agrees with that given by Ellsworth and Beroza (1995) and Beroza and Ellsworth (1996). Because the composite model is phenomenological, *a priori* there is no reason to expect that it can capture the complex nature of the dynamic rupture evolution. Umeda *et al.* (1996), Ellsworth and Beroza (1995), and Beroza and Ellsworth (1996), apparently, are not measuring the time of rupture of the largest subevent. So why this similarity? This similarity may come about if (a) the composite source model of the earthquake, which closely resembles the cascade model (rupture beginning with a small event and progressively breaking larger subevents), captures the gross nature of the dynamic rupture process, and (b) the sudden increase in the velocity ampli-

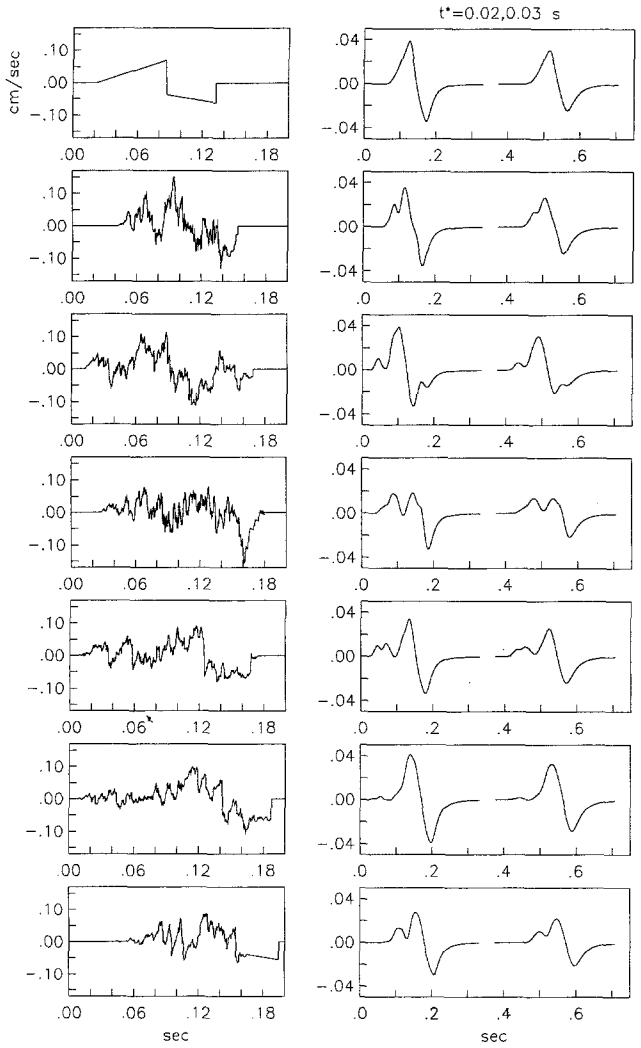

Figure 8. Same as Figure 4 but for M_w = 3.5. The seismograms corresponding to t^* = 0.006 sec is not shown.

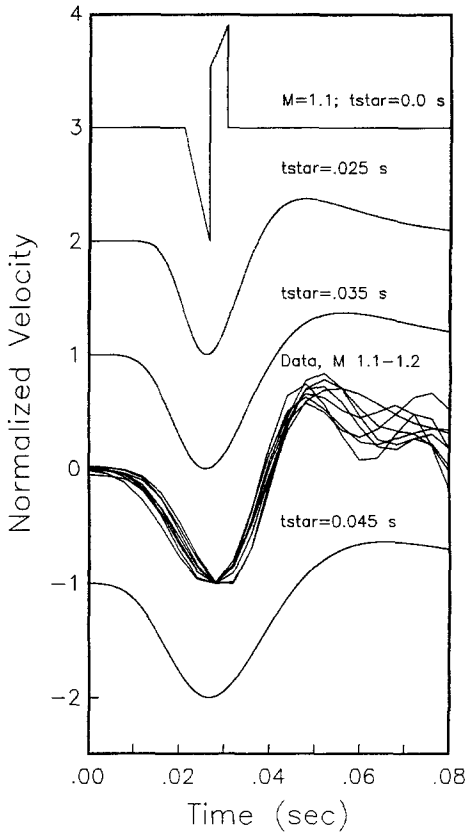

Figure 9. Pulse shapes of synthetic seismograms, M_w = 1.1, from a simple circular source (Sato and Hirasawa, 1973), corresponding to t^* = 0.0, 0.025, 0.035, and 0.045 sec. The seismograms from Zacoalco, Mexico (M_w 1.1 to 1.2) are explained by a t^* ~ 0.04 sec.

tude measured by these authors, generally, corresponds to the rupture of the largest patch. We note that in the composite source model there is no difference between mainshock, aftershocks, and swarm type of activity. Therefore, it cannot explain the absence of the initial phase in aftershocks and swarm type of earthquakes reported by Umeda (1990). However, Umeda's observation does not seem to be universal. For example, several aftershocks of the M = 6.6 earthquake in Figure 3 show this phase. Another example is the Ridgecrest, California, earthquake sequence of 1995 to 1996, which started with an M_L = 5.4 earthquake and included an M_L = 5.8 earthquake (Hauksson *et al.*, 1995). Ellsworth and Beroza (1998) find that all recorded $M \approx 4$ events in the sequence show an initial phase. Thus, we may surmise that the composite source model provides a plausible explanation for the observed initial phase during moderate and large earthquakes. It, however, still remains a puzzle why the prediction from the composite model in Figure 11 fits the data for small earthquakes reported by Iio (1995) so well. We take up this issue in the next section.

Duration of Slow Initial Rise (*t*sip) Observed in Microearthquakes

Iio (1992a, 1995) measured the duration of slow initial rise, *t*sip, in the near-source recordings of the aftershocks of the 1984 Western Nagano Prefecture earthquake and found that *t*sip scaled with M_0 of the earthquake. After extensive analysis and process of elimination, Iio (1995) concluded that *t*sip is related to the source process and can be explained by those models that predict slow slip and rupture velocity following the rupture initiation. Two factors, which were not considered by Iio (1995) in his analysis, are (a) the dependence of *t*sip on M_0 in the presence of attenuation and (b) the possible complexity of microearthquakes. The importance of (a) has already been pointed out by Mori and Kanamori (1996). Here we explore whether (a) and (b) can explain the *t*sip versus Mo data.

The measurements of *t*sip on synthetic seismograms were made following the procedure of Iio (1995). To com-

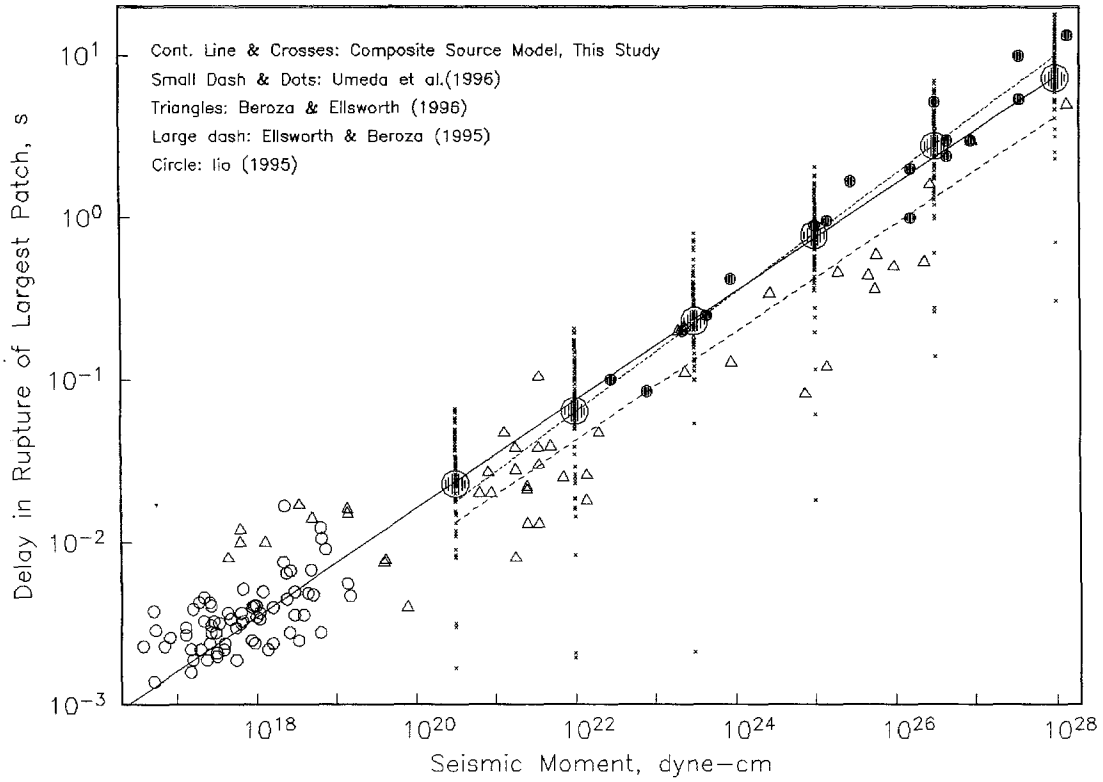

Figure 10. The delay in the rupture of the largest patch measured from the time of rupture initiation, τ, as function of M_0, obtained from different simulations (shown by x) using the composite source model. The median value of 80 simulations (dots) shows that $\tau \propto M_0^{1/3}$. The relationship reported by Umeda *et al.* (1996) between preliminary rupture phase (time interval between rupture initiation and beginning of bright spot) and M_0 is shown by small dashed line. The relation between the duration of the nucleation phase and M_0 given by Ellsworth and Beroza (1995) is shown by large dashed line. Small circles are data on duration of slow initial phase (*t*sip) versus M_0 taken from Iio (1995).

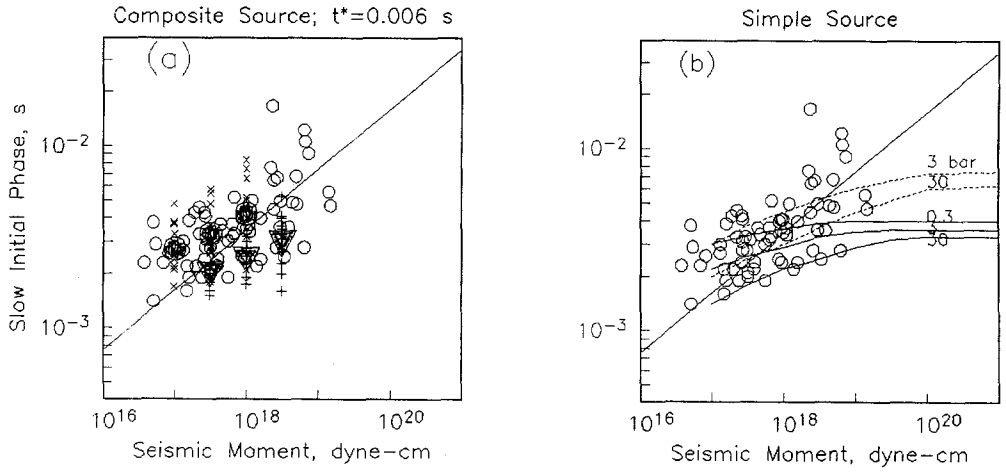

Figure 11. (a) Comparison of the expected *t*sip *versus* M_0 values, computed from the composite source model, with the observed data (circles) of Iio (1995). The calculations have been done for $t^* = 0.006$ sec. Solid circles, $\Delta\sigma = 30$ bars; solid inverted triangles, $\Delta\sigma = 300$ bars. The straight line is the average time delay between the rupture initiation and the breaking of the largest patch according to the composite source model. (b) The predicted *t*sip *versus* M_0 for a simple source model with $t^* = 0.006$ sec (dashed curves) and $t^* = 0.003$ sec (continuous curves) and different values of $\Delta\sigma$.

pare the results of this test directly with Iio's data, we assumed that the ratio of amplitude of the first half cycle of the P wave to the noise on the amplified trace was 60 dB. The onset of the P wave was measured at the point where the signal becomes above the noise on the amplified seismograms. In Figure 11a, the expected $t$sip values computed from the composite source model are compared with the observed $t$sip data of Iio. The calculations have been done for $t^* = 0.006$ sec and $\Delta\sigma = 30$ and 300 bars. The observed data fit well the expected values for $\Delta\sigma = 30$ bars. The predicted $t$sip *versus* M_0 relations for a simple source with $t^* = 0.006$ and 0.003 sec and some values of $\Delta\sigma$ are shown in Figure 11b. We note that the gross trend of the synthetic $t$sip *versus* M_0 curve for $t^* = 0.006$ sec and $\Delta\sigma = 3$ bar is roughly similar to the observations. Figure 11 suggests that it may be possible to explain Iio's $t$sip *versus* M_0 data by a composite or a simple source model and some combination of t^* and $\Delta\sigma$ values. As mentioned earlier, there is some doubt whether these values are well known for the region.

Conclusions

1. Using synthetic seismograms generated from a composite kinematic source model, we find that the observed simplicity of P waves seen in near-source velocity seismograms of small ($M_w < 2$ to 3) earthquakes can, generally, be explained by the attenuation. Thus, the question of whether the sources of such events are simple or complex is not resolvable from much of the existing data, and, hence, the observed simplicity of such events may not be taken as an evidence of breakdown of self-similarity of earthquake rupture process. The only dataset examined by us that suggests simple sources for small earthquakes comes from the studies of Iio (1992a, 1995). Because of small reported attenuation, the complex sources of $M_w \sim 2$ events in this dataset should give rise to complex seismograms. The observed recordings, however, are simple, leading us to the conclude that either the sources of these events were simple or else the local site effects have not been adequately taken in to account.
2. The predicted relationship between the delay in the rupture of the largest patch, measured from the time of its initiation, and the seismic moment of the earthquake in the composite source model is surprisingly close to the relation reported by Umeda *et al.* (1996) and less than a factor of 2 larger than that given by Ellsworth and Beroza (1995) and Beroza and Ellsworth (1996). We note that we did not measure the delay from the synthetic seismograms but computed it for each simulation knowing the point of rupture initiation and the location of the largest subevent. In observed seismograms, this measurement must be difficult to make in an objective fashion. In view of this, the agreement is remarkable. The agreement, for moderate and large earthquakes, may come about if (a) the composite source model of earthquake, which closely resembles the cascade model, captures the gross nature of the dynamic rupture process, and (b) the sudden increase in the velocity amplitude measured by these authors, generally, corresponds to the rupture of the largest patch. Curiously, the prediction from the composite model also fits the data for small earthquakes reported by Iio (1995) very well. Iio (1995) interpreted the time of slow initial phase, $t$sip, *versus* M_0 data as an evidence of slow slip and rupture velocities following the initiation of rupture. We find these data can also be explained by a composite or a simple source model and some combination of t^* and $\Delta\sigma$ values. It is not known, however, whether these values are reasonable for the region.

Acknowledgments

We gratefully acknowledge fruitful discussions with Y. Fukao and T. Sato during their stay in Mexico. The visit of Y. Fukao was made possible by JICA support. H. Kanamori shared many of this thoughts and unpublished manuscripts (and some computer programs) on rupture initiation, and we are very much obliged to him for this and for his patience. The manuscript was revised by W. Ellsworth, Y. Iio, T. Sato, and Y. Umeda. This research was partly supported by CONACYT project 0974PT, DGAPA, UNAM projects IN100795 and IN102494, and the European Union (Contract CH*-CT92-0025).

References

Abercrombie, R. E. (1995). Earthquake source scaling relationships from -1 to 5 M_L using seismograms recorded at 2.5 km depth, *J. Geophys. Res.* **100,** 24015–24036.

Abercrombie, R. E. (1996). The magnitude-frequency distribution of earthquakes recorded with deep seismometers at Cajon Pass, southern California, *Tectonophysics* **261,** 1–7.

Aki, K. (1967). Scaling law of seismic spectrum, *J. Geophys. Res.* **72,** 1217–1231.

Aki, K. (1987). Magnitude frequency relation for small earthquakes: a clue to the origin of f_{max} of large earthquakes, *J. Geophys. Res.* **92,** 1349–1355.

Anderson, J. G. and Q. Chen (1995). Beginnings of earthquakes in the Mexican subduction zone on strong-motion accelerograms, *Bull. Seism. Soc. Am.* **85,** 1107–1115.

Andrews, D. J. (1981). A stochastic fault model, 2, Time-dependent case, *J. Geophys. Res.* **86,** 10821–10834.

Archuleta, R. J., E. Cranswick, C. Muller, and P. Spudich (1982). Source parameters of the 1980 Mammoth Lakes, California, earthquake sequence, *J. Geophys. Res.* **87,** 4595–5006.

Beroza, G. and W. L. Ellsworth (1996). Properties of the seismic nucleation phase, *Tectonophysics* **261,** 209–227.

Cranswick, E., R. Wetmiller, and J. Boatwright (1985). High-frequency observations and source parameters of microearthquakes recorded at hard-rock sites, *Bull. Seism. Soc. Am.* **75,** 1535–1567.

Das, S. and K. Aki (1977). Fault planes with barriers: a versatile earthquake model, *J. Geophys. Res.* **82,** 5648–5670.

Day, S. M. (1982). Three-dimensional simulation of spontaneous rupture: the effect of nonuniform prestress, *Bull. Seism. Soc. Am.* **72,** 1881–1902.

Ellsworth, W. L. and G. C. Beroza (1995). Seismic evidence for an earthquake nucleation phase, *Science* **268,** 851–855.

Ellsworth, W. L. and G. C. Beroza (1998). Observation of the seismic

nucleation phase in the Ridgecrest. California, earthquake sequence, *Geophys. Res. Lett.* **25,** 401–404.

Frankel, A. (1991). High-frequency spectral falloff for earthquakes, fractal dimension of complex rupture, b-value, and the scaling of strengths on faults, *J. Geophys. Res.* **96,** 6291–6302.

Fullerman, W. I. (1962). Dispersive body waves, *J. Geophys. Res.* **67,** 5279–5291.

Hanks, T. C. (1979). b-values and $\omega^{-\gamma}$-seismic source models: implications for tectonic stress variations along active crustal fault zones, and the estimation of high-frequency strong ground motion, *J. Geophys. Res.* **84,** 2235–2242.

Hauksson, E., K. Hutton, H. Kanamori, L. Jones, J. Mori, S. Hough, and G. Roquemore (1995). Preliminary report on the 1995 Ridgecrest earthquake sequence in the eastern California, *Seism. Res. Lett.* **66,** 54–60.

Hough, S. E., J. G. Anderson, J. Brune, F. Vernon III, J. Berger, J. Fletcher, L. Haar, T. Hanks, and L. Baker (1988). Attenuation near Anza, California, *Bull. Seism. Soc. Am.* **78,** 672–691.

Iio, Y. (1992a). Slow initial phase of the P-wave velocity pulse generated by microearthquakes, *Geophys. Res. Lett.* **19,** 477–480.

Iio, Y. (1992b). Seismic source spectrum of microearthquakes, *Bull. Seism. Soc. Am.* **82,** 2391–2409.

Iio, Y. (1995). Observations of the slow initial phase generated by microearthquakes: implications for earthquake nucleation and propagation, *J. Geophys. Res.* **100,** 15333–15349.

Keilis-Borok, V. (1959). On estimation of estimation of the displacement in an earthquake source and of source dimensions, *Ann. Geofis. (Rome)* **12,** 205–214.

Madariaga, R. (1976). Dynamics of expanding circular fault, *Bull. Seism. Soc. Am.* **66,** 639–666.

Matsu'ura, M., H. Kataoka, and B. Shibazaki (1992). Slip-dependent friction law and nucleation processes in earthquake rupture, *Tectonophysics* **211,** 135–148.

Mikumo, T. and T. Miyatake (1978). Dynamic rupture process on a three-dimensional fault with non-uniform frictions and near-field seismic waves, *Geophys. J. R. Astr. Soc.* **59,** 496–522.

Mikumo, T. and T. Miyatake (1987). Numerical modelling of realistic fault rupture processes, in *Seismic Strong Motion Synthetic,* Chap. 3, Academic, New York, 91–151.

Mikumo, T. and T. Miyatake (1995). Heterogeneous distribution of dynamic stress drop and relative fault strength recovered from results of waveform inversion: the 1984 Morgan Hill, California, earthquake, *Bull. Seism. Soc. Am.* **85,** 178–193.

Miyatake, T. (1980). Numerical simulations of earthquake source process by a three-dimensional crack model, Part I. Rupture process, *J. Phys. Earth* **28,** 565–598.

Mori, J. and H. Kanamori (1996). Initial rupture of earthquakes in the 1995 Ridgecrest. California, sequence, *Geophys. Res. Lett.* **23,** 2437–2440.

Papageorgiou, A. S. and K. Aki (1983). A specific barrier model for the quantitative description of inhomogeneous faulting and the prediction of strong ground motion. I: Description of the model; II: Application of the model; *Bull. Seism. Soc. Am.* **73,** 693–722, 953–978.

Sato, T. and T. Hirasawa (1973). Body wave spectra from propagating shear cracks, *J. Phys. Earth* **21,** 415–431.

Sibazaki, B. and M. Matsu'ura (1992). Spontaneous processes for nucleation, dynamic propagation, and stop of earthquake rupture, *Geophys. Res. Lett.* **19,** 1189–1192.

Singh, S. K., M. Ordaz, M. Rodriguez, R. Quaas, E. Mena, M. Ottaviani, J. G. Anderson, and D. Almora (1989). Analysis of near-source strong motion recordings along the Mexican subduction zone. *Bull. Seism. Soc. Am.* **79,** 1697–1717.

Umeda, Y. (1990). High-amplitude seismic waves radiated from the bright spot of an earthquake, *Tectonophysics* **175,** 81–92.

Umeda, Y. (1992). The bright spot of an earthquake, *Tectonophysics* **211,** 13–22.

Umeda, Y., T. Yamashita, T. Tada, and N. Kame (1996). Possible mechanisms of dynamic nucleation and arresting of shallow earthquake faulting, *Tectonophysics* **261,** 179–192.

Umino, N. and I. S. Sacks (1993). Magnitude-frequency relations for northeastern Japan. *Bull. Seism. Soc. Am.* **83,** 1492–1506.

Yamashita, T. and Y. Umeda (1994). Earthquake rupture complexity due to dynamic nucleation and interaction of subsidiary faults, *Pageoph* **143,** 89–116.

Zeng, Y., J. G. Anderson, and G. Yu (1994). A composite source model for computing realistic synthetic strong ground motions, *Geophys. Res. Lett.* **21,** 725–728.

Instituto de Geofísica
UNAM, C.U.
04510 Mexico D.F., Mexico
(S.K.S., T.M., J.P., C.V.)

Instituto de Ingeniería
UNAM, C.U.
04510 Mexico D.F., Mexico
(M.O.)

National Geophysical Research Institute
Hyderabad 500007, India
(P.M.)

Manuscript received 14 November 1997.